PROCEEDINGS OF THE YEREVAN STATE UNIVERSITY

Physical and Mathematical Sciences 2017, **51**(1), p. 81–84

Physics

COMPARATIVE ANALYSIS OF TWO DIFFRACTION SCHEMES FOR WIDELY DIVERGENT BEAM OF X-RAY RADIATION

K. T. AVETYAN, L. V. LEVONYAN [*], H. S. SEMERJYAN

Chair of Solid State Physics YSU, Armenia

Comparative analysis of two diffraction schemes *d-c* (diaphragm-crystal) and *c-d* (crystal-diaphragm) for widely divergent beam of X-ray radiation is conducted. It is justified that in *c-d* scheme the diffraction image is a topographic map of the studied area of the crystal.

***Keywords*:** X-ray radiation, widely divergent beam, diffraction scheme, topographic map.

Introduction. The diffraction image, formed by widely divergent beam (WDB) of the characteristic X-ray radiation, contains broad information on the peculiarities of the crystal structure of the studied object, since a large number of Bragg reflections are being registered simultaneously. Currently, there are two basic ways for implementing the X-ray WDB diffraction: the Kossel method, when the X-ray point source is located on the surface (or under the surface) of the object, and the pseudo-Kossel method, when the point source is located above the surface of the object [1–3]. Methods differ in the way of exciting the characteristic radiation and in creating a radiation point source. We have used two slightly different schemes for implementing the WDB diffraction using a standard radiation source: an X-ray tube with a linear focal spot [4, 5]. In one of the schemes the X-ray radiation passes through the diaphragm (a cone-shaped hole with the diameter of 30–50 μm in the tantalum plate) and falls on the studied crystal. On the photographic plate mounted behind the crystal, only the diffracted radiation falls. The primary (non-diffracted) radiation is captured by trap [4]. The diaphragm, the crystal and the photographic plate are placed in a small chamber, which rotates around the diaphragm axis during the exposure. This scheme is called *d-c* (diaphragm-crystal) (Fig. 1, a). In the *d-c* scheme the diaphragm acts as a point source. When the diaphragm is installed close to the sample (before or after the sample), the scheme is similar to the Kossel scheme, and the diffraction image does not differ from the classical Kossel pattern. When the diaphragm is installed at a distance of 2–3 *mm* and more, the scheme is similar to the WDB scheme, and the diffraction image is similar to the pseudo Kossel pattern. Thus, a relatively simple scheme allows to obtain both, a Kossel pattern and a pseudo Kossel pattern of the same sample. The difference between such diffraction images is that the Kossel patterns are formed on the local region of the studied crystal, determined by the diameter of the diaphragm, and they do not represent a topographic map of the test sample, while the pseudo Kossel pattern is formed on a relatively large area of the studied crystal. However,

[*] E-mail: llevonyan@ysu.am

such a diffraction image, as we will see later, also does not represent a topographic map of the investigated region of the crystal.

In the *d-c* scheme, as has been said earlier, the primary (non-diffracted) radiation is captured by trap and does not reach the photographic plate. Such a scheme allows to examine samples of very small sizes.

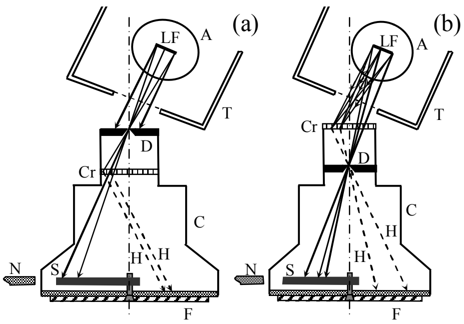

Fig. 1. Experiment diagram: T is X-ray tube; A is anode; LF is linear focus; C is chamber; Cr is studied crystal; D is diaphragm; S is immovable valve; F is photographic plate; N is permanent magnet; H is diffracted radiation.

(a) *d-c* and (b) *c-d* schemes.

In another scheme the investigated crystal is being "irradiated" by divergent X-rays, so that at any point of investigated area of the crystals the Bragg condition is satisfied for several families of atomic planes simultaneously (multiwave diffraction) (Fig. 1, b) [5].

A diaphragm is set after the crystal at a distance of 2–5 *mm*. On the photographic plate, mounted after the diaphragm, only the diffracted light passing through the diaphragm falls. The primary (non-diffracted) radiation is captured by trap, which does not change its position relative to the radiation source when the chamber is rotating. As far as for the specified family of planes (hkl), and for the given wavelength of the characteristic radiation the diffraction angle is defined, then the radiation diffracted at certain points of the crystal can pass through the diaphragm. We call these points as active points, and the scheme is called *c-d* scheme. To the best of our knowledge, there is no in literature any analogue to our *c-d* scheme.

Comparison of Schemes. Distribution of active points on the surface of the crystal is determined by the following requirement: the radiation diffracted at the active point $M(x,y,z)$ of the crystal surface passes through the diaphragm. If the beginning of the rectangular coordinate system is superposed with the center of the diaphragm, z-axis with the normal to the photographic plate (the diaphragm axis), then for the active points we will have

$$x_1\cos\alpha + y_1\cos\beta + z_1\cos\gamma = -\sqrt{x_1^2+y_1^2+z_1^2}\,\sin\theta_{hkl},$$

where $\alpha,\ \beta,\ \gamma$ are angles between the direction $[hkl]$ and the coordinate axes. This is the equation for conical surfaces where axes coincide with the $[hkl]$ directions, and the top is common for all the families of the (hkl) atomic planes and coincides with the center of the diaphragm. For the cross-section of the conical surfaces by the plane $z_1 = 1$ (the outer face of the crystal), we will get

$$x_1^2(\cos^2\alpha - \sin^2\theta) + 2x_1y_1\cos\alpha\cos\beta + y_1^2(\cos^2\beta - \sin^2\theta) +$$
$$+2x_1 l\cos\alpha\cos\gamma + 2y_1 l\cos\beta\cos\gamma + l^2(\cos^2\gamma - \sin^2\theta) = 0.$$

This means that the active points will be distributed on the hyperbolas. Conical surfaces extend unrestrictedly in both directions from the top so that they intersect the plane $z = -L$, where the photographic plate is installed. The diffraction image formed on the photographic plate is also a set of conic sections. Between the distribution of active points on the surface of the crystal and the distribution of the diffraction maximum on the photo plate there is one-to-one correspondence, i.e. each active point $M_1(x_1,\ y_1)$ on the crystal surface has a corresponding point $M(x,\ y)$ on the diffraction image. Otherwise, the image generated through such scheme is a magnified image or a topographic map of the active points distribution.

In the *d-c* scheme the crystal is irradiated by the diverging beam emanating from the diaphragm that acts as a point source mounted above the crystal. However, between the distribution of active points on the surface of the crystal and the distribution of the diffraction maximum on the photo plate there is no one-to-one correspondence. In other words, the diffraction image is not a topographic map of the part of crystal under investigation [1].

Let us consider the essential difference between *c-d* and *d-c* schemes. In *c-d* scheme any point of the crystal part under examination is illuminated by the radiation in broad angular limits, hence, the diffraction at all points will be multiwave. Radiation diffracted at any plane (hkl) has a well-defined direction. Therefore, if one of the diffracted waves, emanating from the given active point, passes through the diaphragm, then another wave emanating from the same point cannot pass through the diaphragm. Hence, it could be stated that in *c-d* scheme the diffraction image is formed only by one diffracted wave, i.e. each point of the diffraction image receives information from only one corresponding active point. In other words, the multiwave character of the diffraction is not manifested. Consequently, the diffraction image in *c-d* scheme represents a topographic map of the active points on the crystal surface.

The multiwave character of the diffraction in a *d-c* scheme is manifested in the fact that all the diffracted waves reach the photographic plate without restriction. In this case the given point of the diffraction image is reached by the waves diffracted at different active points of the crystal, i.e. the information superposition takes place. Therefore, the diffraction image in this case could not represent a topographic map of the investigated crystal.

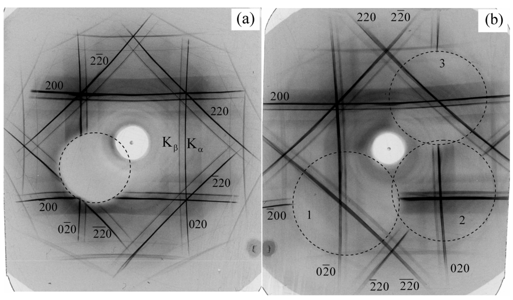

Fig. 2. Diffraction images of the crystal LiF obtained in:
(a) *c-d* and (b) *d-c* schemes.

Experiment and Conclusion. Fig. 2, a shows the diffraction image of the crystal LiF formed by the MoK_α and K_β characteristic radiations and obtained in the *c-d* scheme. The intense lines are hyperbolas generated by the K_α radiation, the less intense lines are generated by the K_β radiation. The white circle in the center is the “shadow” of the roller, which holds the trap of the primary (non-diffracted) beam. In the crystal, shaped as a 0.5 *mm* thick plate, a hole of 0.8 *mm* in diameter is made. The large face of the crystal, the plane (001), is oriented parallel to the photographic plate. The crystal is mounted in a way that the “image” of a hole in Fig. 2, a falls on the intersection of the hyperbolas generated by the reflections $(\bar{2}00)$, $(0\bar{2}0)$ and $(\bar{2}\bar{2}0)$ $\big($the center of the hole coincides with the unit $[[\bar{2}\bar{2}0]]\big)$. The image of the hole (the white circle) is clearly notable on the diffraction pattern. As seen in the Fig. 2, within the range of that circle the hyperbolas $(\bar{2}00)$, $(0\bar{2}0)$ and $(\bar{2}\bar{2}0)$, and are interrupted, which testifies that in the *c-d* scheme the information reaches this circle area only from the vicinity of the lattice site $[[\bar{2}\bar{2}0]]$ having the size of the hole. The information from other parts of the crystal does not arrive at this point of the image. Hereby, it can be stated that in the *c-d* scheme there is one-to-one correspondence between the distribution of active points on the surface of the crystal and the distribution of the diffraction maximum in the image, i.e. the diffraction image represents a topographic map of the active points.

Fig. 2, b shows the diffraction image of the same crystal LiF obtained in the *d-c* scheme. The mutual alignment of the hole in the crystal and the diaphragm is kept unchanged, i.e. the crystal unit, coinciding with the center of the hole, corresponds to the crystal lattice site $[[\bar{2}\bar{2}0]]$. As it can be seen in the diffraction pattern, a distinct "image" of the hole is not formed. Existence of the hole manifests itself in three different locations of the diffraction pattern. At the area 1 (vicinity of the reflex $[[\bar{2}\bar{2}0]]$ in the Fig. 2) the hyperbola $(\bar{2}00)$ is interrupted, at the area 2 (vicinity of the reflex $[[\bar{2}20]]$) the hyperbola $(\bar{2}20)$ is interrupted, and at the area 3 (vicinity of the reflex [[220]]) the hyperbola (020) is interrupted.

It follows that in the *d-c* scheme, at a given location of the diaphragm and the hole in the crystal, the radiation diffracted from the zone within the crystal, where the hole is drilled, arrives at three different areas of the diffraction image. Conversely, to many areas of the diffraction image the information comes from different parts of the crystal. This means that in the *d-c* scheme superposition of the information takes place.

Received 22.12.2016

REFERENCES

1. **Leader V.V.** X-Ray Divergent-Beam (Kossel) Technique: A Review. // Crystallography Reports, 2011, v. 56, p. 169.
2. **Aristov V.V., Shechtman V.S., Shmytko I.M.** Precise Measurement of Crystallographic Parameters by the Method of Widely Divergent X-Ray Beam. // Kristallografiya, 1973, v. 18, p. 706 (in Russian).
3. **Aristov V.V., Shechtman V.S., Shmytko I.M.** Peculiarities of the Optical Scheme of Widely Divergent X-Ray Beam. // Kristallografiya, 1976, v. 21, p. 50 (in Russian).
4. **Avetyan K.T., Levonyan L.V., Semerjyan H.S., Arakelyan M.M., Badalyan O.M.** Specific Features of Two Diffraction Schemes for a Widely Divergent X-Ray Beam. // Crystallography Reports, 2015, v. 60, p. 207.
5. **Avetyan K.T.** New Aspect of Diffraction of a Highly Divergent Characteristic X-Ray Beam. // Crystallography Reports, 2010, v. 55, p. 737.